An important role of G638 in the *cis*-cleavage reaction of the *Neurospora* VS ribozyme revealed by a novel nucleotide analog incorporation method

DOMINIC JAIKARAN, M. DUANE SMITH, REZA MEHDIZADEH, JOAN OLIVE, and RICHARD A. COLLINS
Department of Molecular Genetics, University of Toronto, Toronto, Ontario M5S 1A8, Canada

ABSTRACT

We describe a chemical coupling procedure that allows joining of two RNAs, one of which contains a site-specific base analog substitution, in the absence of divalent ions. This method allows incorporation of nucleotide analogs at specific positions even into large, *cis*-cleaving ribozymes. Using this method we have studied the effects of substitution of G638 in the cleavage site loop of the VS ribozyme with a variety of purine analogs having different functional groups and pK_a values. Cleavage rate versus pH profiles combined with kinetic solvent isotope experiments indicate an important role for G638 in proton transfer during the rate-limiting step of the *cis*-cleavage reaction.

Keywords: ribozyme mechanism; RNA ligation; general acid–base catalysis

INTRODUCTION

The early observation that the small self-cleaving ribozymes (hammerhead, hairpin, hepatitis delta virus [HDV], and *Neurospora* Varkud satellite [VS]), typically, exhibit their maximal observed cleavage rates in the presence of divalent cations led to the proposal that these ribozymes were inherently metalloenzymes (Pyle 1993). Subsequent experiments showed that these ribozymes are capable of substantial cleavage rates even in the absence of divalent cations (Nesbitt et al. 1997; Young et al. 1997; Murray et al. 1998; Curtis and Bartel 2001; O'Rear et al. 2001; Perrotta and Been 2006; Poon et al. 2006), inspiring a broader search for alternative or additional catalytic strategies. During the past few years evidence has emerged that many ribozymes use general acid–base catalysis to cleave and/or ligate specific phosphoester linkages; however, identifying the exact roles of individual nucleotides in the chemical mechanism is still an ongoing process (Nakano et al. 2000; Pinard et al. 2001; Shih and Been 2001; Bevilacqua 2003; Bevilacqua et al. 2004; Ke et al. 2004; Das and Piccirilli 2005; Fedor and Williamson 2005; Han and Burke 2005; Perrotta et al. 2006; Wilson et al. 2006; Sigel and Pyle 2007).

Nucleotide analogs have proven very useful in investigating the roles of individual base, sugar, and phosphate functional groups in the function of an RNA. Interference approaches, in which an analog is incorporated during in vitro transcription into random positions at low frequency in a population of RNA molecules, have been used to rapidly identify positions important for folding and/or catalysis in a variety of RNAs (Eckstein 1985; Strobel 1999). Other experimental designs require a pure population of RNA molecules containing an analog introduced at one or more specific positions; this is usually accomplished by chemical synthesis (Ogilvie et al. 1988; Scaringe et al. 1990; Wincott et al. 1995). Such site-specific substitution has been used to incorporate analogs with altered functional properties for studies of RNA structure, folding and catalysis (for review, see Baum and Silverman 2007). Due to limitations of chemical synthesis, efficient site-specific incorporation is applicable only to RNAs up to about 60 nucleotides. To study larger RNAs, the short chemically synthesized RNA can sometimes be annealed with other RNAs to reconstitute a complex that is intended to mimic the important aspects of the structure of the larger, natural unimolecular *cis* RNA. However, the reannealed complex does not always completely recapitulate the properties of the unimolecular RNA.

Reprint requests to: Richard A. Collins, Department of Molecular Genetics, University of Toronto, Toronto, ON M5S 1A8, Canada; e-mail: rick.collins@utoronto.ca; fax: (416) 978-6885.

Article published online ahead of print. Article and publication date are at http://www.rnajournal.org/cgi/doi/10.1261/rna.936508.

Another approach to incorporating site-specific analogs into large RNAs involves enzymatically ligating the chemically synthesized RNA to the flanking region(s) of the larger RNA (which has been produced separately, either by chemical synthesis or in vitro transcription) to obtain the desired full-length RNA. Typically, the two RNAs are brought together by a complementary DNA bridging molecule and joined using either T4 DNA ligase or T4 RNA ligase (Moore and Sharp 1992; Moore and Query 2000). Silverman and coworkers recently reported a different approach in which a ribozyme catalyzes ligation of the two RNAs (Baum and Silverman 2007). All of these RNA ligation methods require long incubation times and the presence of Mg^{2+}, conditions that are incompatible with obtaining uncleaved precursor RNA from fast-cleaving ribozymes. In special situations it has been possible to manipulate experimental conditions to allow ribozyme-mediated ligation of the short chemically synthesized oligonucleotide containing the base analog to the rest of the RNA (Hiley et al. 2002); however, a general approach for incorporating nucleotide analogs into uncleaved precursor RNAs of the larger ribozymes has been lacking.

Here we report the development of a method for joining two RNAs in the absence of Mg^{2+}. We use this method to evaluate the effects of purine nucleotide analog substitution at position G638 in the cleavage loop of the VS ribozyme on the kinetics and mechanism of the *cis*-cleavage reaction.

RESULTS

We have previously found that the fast-cleaving version of the VS ribozyme, designated RG (Fig. 1A), exhibits pH- and D_2O-dependent cleavage between pH 5 and 9, consistent with a catalytic mechanism that utilizes general acid–base catalysis (Zamel et al. 2004). A756 in helix VI has been implicated as one probable participant in the chemical step (Lafontaine et al. 2001b, 2002; Hiley et al. 2002; Sood and Collins 2002; Jones and Strobel 2003; Smith and Collins 2007). Previous studies have pointed to G638, in the cleavage loop of stem–loop I, as also being important for cleavage and/or ligation of the VS ribozyme: this nucleotide is strongly conserved in ligation-based in vitro selection experiments (Andersen and Collins 2000); mutation to any other base strongly decreases activity in a *trans*-cleaving version of the ribozyme (Wilson et al. 2007), and NMR studies of stem–loop I show G638 to be close enough to the scissile bond to potentially affect the chemical step of the reaction (Hoffmann et al. 2003).

Site-directed mutagenesis of position 638

Figure 1B shows the effect of mutation of G638 to each of the other natural nucleobases on the pH-rate profile of the *cis*-cleaving RG version of the VS ribozyme. The 638C and 638U mutants cleave very slowly and are unaffected by pH;

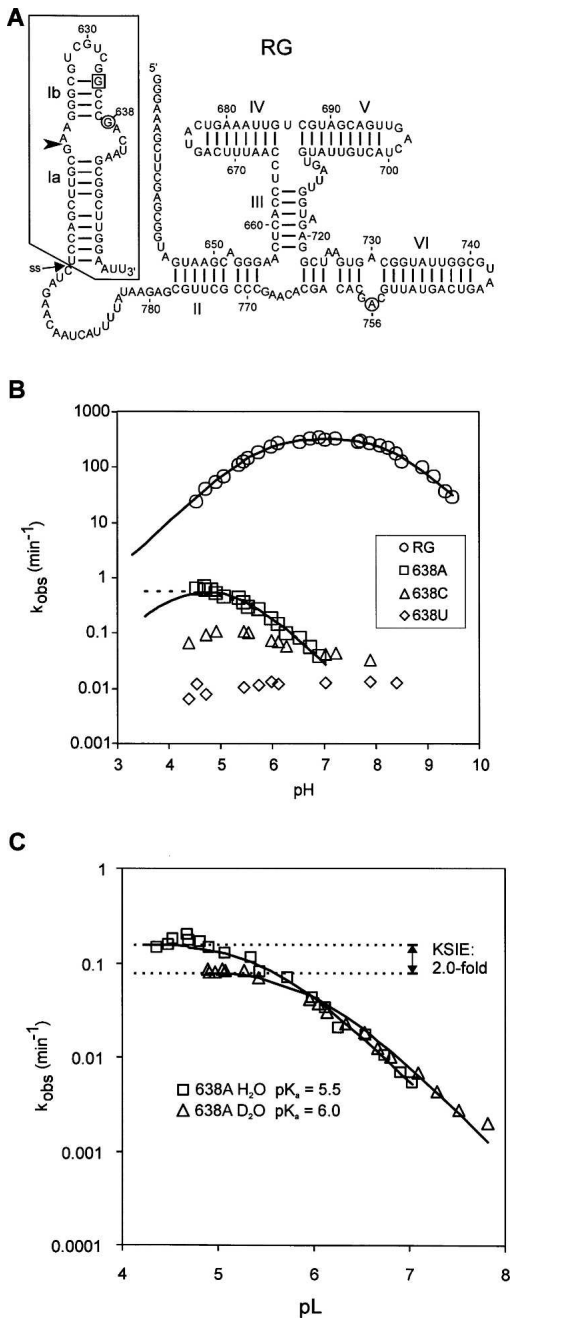

FIGURE 1. Site-directed mutagenesis of position 638 in the RG version of the VS ribozyme. (*A*) Secondary structure of RG self-cleaving precursor RNA. The cleavage site is indicated by the arrowhead; the G634C substitution that enforces the active conformation of helix Ib is boxed. The putative nucleobases involved in general acid–base catalysis, G638 and A756, are circled. To incorporate nucleotide analogs at position 638 the boxed region was synthesized chemically and joined via disulfide linkage at the position indicated by the arrow labeled "ss" (see Fig. 3). (*B*) The effect of pH on the apparent cleavage rate constant (k_{obs}) of wild-type and mutant RNAs with the indicated base substitutions at position 638. Where appropriate, data are fit to a model of general acid–base catalysis (solid line) or general acid-only catalysis (dashed line). Estimates of kinetic parameters are summarized in Table 1. (*C*) Kinetic solvent isotope effect on cleavage of the 638A mutant. k_{obs} in H_2O (squares) or D_2O (circles) versus pL (pH or pD, respectively).

these mutants were not investigated further. In contrast, the 638A mutant exhibits a distinctive rate versus pH curve that could be interpreted in at least two ways. The simplest interpretation is that this curve describes a reaction catalyzed only by a general acid with an apparent pK_a of 5.5 (Fig. 1B, dashed line), i.e., mutation of G638 to adenosine eliminates the contribution of the general base. Alternatively, the data could be fit to a general acid–base model with one apparent pK_a of 5.3 and the other shifted below the pH range in which we had collected data (<4.5) (Fig. 1B, solid line). A kinetic solvent isotope effect (KSIE) of twofold on the plateau of the curve and a rightward shift of 0.5 units in the rate versus pL curve for reactions performed in D_2O provide evidence that proton transfer is still the rate-limiting step in the 638A mutant (Fig. 1C). As with the wild type (Smith and Collins 2007), the magnitude of the KSIE is too small for proton inventory experiments to convincingly distinguish between transfer of one or two protons in the rate-limiting step (data not shown). Taken together, these data indicate that the identity of the nucleobase at position 638 strongly influences the rate-limiting proton transfer step of the cleavage reaction.

Cleavage activity decreases sharply below pH 4

In an attempt to distinguish between a general acid–base and general acid-only mechanism in the 638A mutant, we measured cleavage rates of wild type and 638A at even lower pH. The data in Figure 2A show that below about pH 4 the rate versus pH curves of both RNAs decrease extremely steeply, indicative of the involvement of an additional process in the overall observed cleavage reaction (see Discussion). Because the steep slope of this part of the rate versus pH curve was likely to have an impact on our ability to accurately estimate apparent pK_a s in the lower pH region of the bell-shaped portion of the curve, we constructed a mathematical model to describe the rapid decrease in rate at low pH (see Materials and Methods). A steep decrease in k_{obs} versus pH could be explained by (1) an ''independent sites'' model in which a ribozyme molecule is inactivated by independent protonation of any one of several nucleobases (Knitt and Herschlag 1996) or (2) a ''cooperative crash'' model in which protonation of one nucleobase increases either the probability of protonation of another nucleobase or the probability that such protonation will lead to loss of activity. In these models, the active and inactive states of the RNA are assumed to be in rapid equilibrium relative to the intrinsic rate of the cleavage step, k_1. Each model postulates some number, n, of relevant nucleobases, each with an average apparent pK_a, pK_a^C, which when protonated causes loss of activity; however, the predicted shapes of the rate versus pH curves for each model are fundamentally different for the two models (Fig. 2B,C).

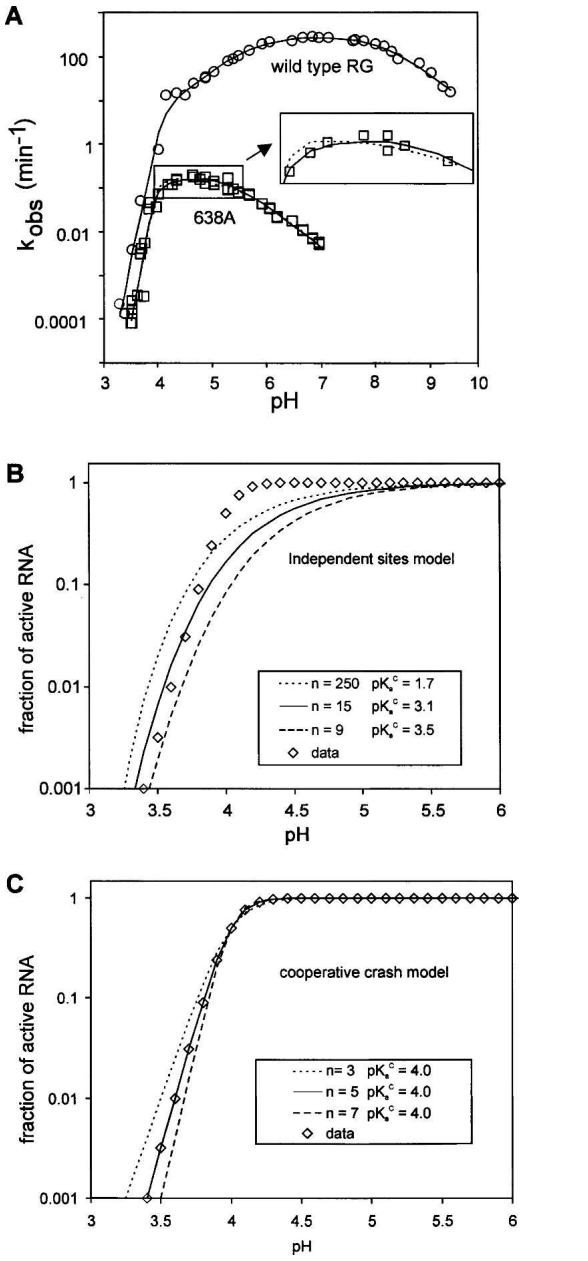

FIGURE 2. Steep loss of self-cleavage activity at low pH. (*A*) The effect of low pH on k_{obs} for wild type (circles) or G638A (squares). Data are fit to a model that combines the cooperative crash with general acid–base catalysis (solid lines) or with general acid-only catalysis (dotted line); see Materials and Methods. The *inset* is an enlargement with some data points removed to allow visualization of the two different fit lines. (*B*,*C*) Simulations showing the difference in shapes of the curves and the effects of parameter values for n and pK_a^C for the independent sites (*B*) or cooperative crash (*C*) models (Equations 4 and 5 in Materials and Methods). Data (diamonds) were simulated with the cooperative crash model (n = 5, pK_a^C = 4.0; where n represents the number of nucleobases, each with an apparent pK_a, pK_a^C, that must be protonated to inactivate the ribozyme) and fit to Equation 4 or 5. Solid lines show the best fit solution using each model; additional lines are simulations with the specified values for n and pK_a^C.

We fit the wild-type rate versus pH data to equations describing the standard general acid–base model (Equation 4) combined with either the independent or cooperative models (Equation 6 or 7). The independent sites model did not qualitatively fit the data, even with extreme, biologically unreasonable parameter values (data not shown). In contrast, the cooperative model produced a good fit with optimal values of $n = 5$ and $pK_a^C = 4.1$ (Fig. 2A, solid line). Slightly higher or lower values of pK_a^C ($\pm\sim0.1$ pH units) also fit the data almost equally well if the value of n was adjusted to compensate ($\pm\sim0.5$). This analysis suggests that the wild-type ribozyme is rate-limited by general acid–base catalysis in the pH range from 4.5 to 9, and rapidly loses activity at lower pH due to a phenomenon resulting from cooperative protonation of approximately five bases with apparent $pK_a \approx 4$.

A similar analysis of the rate versus pH curve for 638A also showed that the steep loss in activity below pH 4 did not fit to the independent sites model (not shown) but did fit to the cooperative crash model. Combining the cooperative crash model with a general acid-only model is sufficient to explain the complete rate versus pH curve for 638A with an apparent $pK_a^A = 5.5$ for the general acid, and $n = 6.7$ and $pK_a^C = 4.0$ (Fig. 2A dotted line). However, the data are also consistent with a general acid–base model with one apparent pK_a of 5.3 and a hypothetical second titratable group with $pK_a \approx 4.1$ (Fig. 2A, solid line: the solid and dotted lines are almost superimposable; kinetic parameters are summarized in Table 1). The estimate of the latter pK_a is unlikely to be accurate, as this part of the rate versus pH curve is strongly affected by the steep decrease in activity caused by the cooperative inactivation involving multiple functional groups with an apparent $pK_a^C \approx 4.0$ very similar to the predicted pK_a of the second hypothetical general acid–base group (see Discussion). Even though these two models cannot be distinguished, the large change in rate versus pH curve observed with the 638A mutant further supports the hypothesis that the nucleobases at position 638 plays an important role in the rate-limiting proton transfer step of the *cis*-cleavage reaction.

A novel chemical ligation method to incorporate site-specific nucleotide analogs

To further investigate the role in catalysis of the nucleobases at position 638, we needed a way of selectively replacing this nucleobase with nonnatural analogs. As described in the Introduction, currently available methods require Mg^{2+}-containing buffers that are incompatible with obtaining uncleaved precursor RNA from a fast-cleaving ribozyme such as RG. We were aware of one chemical ligation procedure that could join two modified RNAs via reductive amination in the absence of Mg^{2+}; however, the long reaction times reported (up to 7 d) were impractical for our needs (Bellon et al. 1996). Our attempts to improve on this procedure were unsuccessful. A completely different chemistry, using a sulfhydryl-containing nucleotide to attack a nucleotide containing an activated disulfide, has been used to monitor tertiary structure within an RNA (Cohen and Cech 1997). By combining the best features of these two chemical approaches we have designed a strategy that joins two RNAs via a disulfide bond.

Our general approach is diagrammed in Figure 3A. Molecule 1 (the ''upstream'' RNA) represents any RNA whose 3′ end is to be joined to the 5′ end of molecule 5 (the ''downstream'' RNA). Molecule 1 is first converted to molecule 2 via oxidation with sodium periodate, then to molecule 3 via reaction with hexamethylenediamine and sodium cyanoborohydride. A sulfhydryl reactive moeity is introduced onto the 3′ amine of Molecule 3 by reaction with N-succinimidyl 3-(2-pyridyldithiol)propionate (SPDP) to make molecule 4. The downstream RNA, molecule 5, contains a 5′ SH group, prepared by chemical synthesis (although priming T7 transcription with a dinucleotide containing a 5′ sulfhydryl group may also work). When the upstream and downstream RNAs are mixed together the 5′SH group in molecule 5 attacks the sulfhydryl reactive moiety in molecule 4, joining the two RNAs via a disulfide bond to make molecule 6, the full-length RNA (Fig. 3A,B).

To determine if the disulfide linkage itself had any effect on the kinetic properties of the VS ribozyme we compared cleavage time courses of the wild-type RG ribozyme that had been synthesized by in vitro transcription to those of the equivalent molecule obtained by joining a chemically synthesized stem–loop I to the rest of the ribozyme that had been synthesized by in vitro transcription. The disulfide-linked RNA is designated RGssG, where the last G indicates that guanosine is present at position 638; RNAs containing base analogs at position 638 are named in a parallel fashion (see the following section). The apparent first-order cleavage rate constant of RGssG under standard reaction conditions was the same within experimental error of that of RG synthesized by T7 transcription (3.6 versus 4.0 sec^{-1}; data not shown). The extents of cleavage of RGssG and its nucleotide analog containing variants (described below) were somewhat lower than for in vitro transcribed RG RNA (about 60% versus 85%): chase experiments (Zamel et al. 2004) provided no evidence that this was due to an altered cleavage-ligation equilibrium; denaturing gel purification of the uncleaved RGssG RNA followed by renaturation indicated that a portion of the inactive RNA was misfolded, and suggested that the remainder may have been inactivated by side reactions during synthesis (data not shown). Comparison of the first order cleavage rate constant of the active population of the RNA versus pH for RG and RGssG showed that apparent cleavage rate constants of the two RNAs were very similar over the pH range examined, supporting the conclusion that the

TABLE 1. Summary of kinetic parameters

RNA	Maximum k_{obs} (min^{-1})	Fold reduction in maximum k_{obs}	General acid-only + crash				General acid–base + crash									
											k_1 (min^{-1})		Ratio of k_1^{wt}:k_1^{mutant} for all combinations of models 1 and 2			
			pK_a^A	pK_a^C	n	k_1 (min^{-1})	pK_a^A	pK_a^B	pK_a^C	n	Model 1	Model 2	$\frac{\text{Model1}}{\text{Model1}}$	$\frac{\text{Model2}}{\text{Model2}}$	$\frac{\text{Model1}}{\text{Model2}}$	$\frac{\text{Model2}}{\text{Model1}}$
RG (wild type)	262	1	N/A				5.8	8.3	4.1	5.0	292	93,600	N/A	N/A	N/A	N/A
638A	0.16	1638	5.5	4.0	6.7	0.17	4.1	5.3	4.0	6.4	0.25	3.8	1168	24,632	77	374,400
RGssDAP	0.6	437	6.8	4.3	3.7	0.5	4.8	6.5	4.0	6.5	0.8	47	365	1991	6	117,000
RGssI	12	22	N/A				5.7	7.9	N/D	N/D	14.8	2600	20	36	0.11	6324
RGss2AP	0.05	5240	N/A									N/A				
RGssP	0.01	26,200	N/A									N/A				

N/A, not applicable; N/D, not determined. See Materials and Methods for definitions of parameters and Figure 5 for explanation of models.

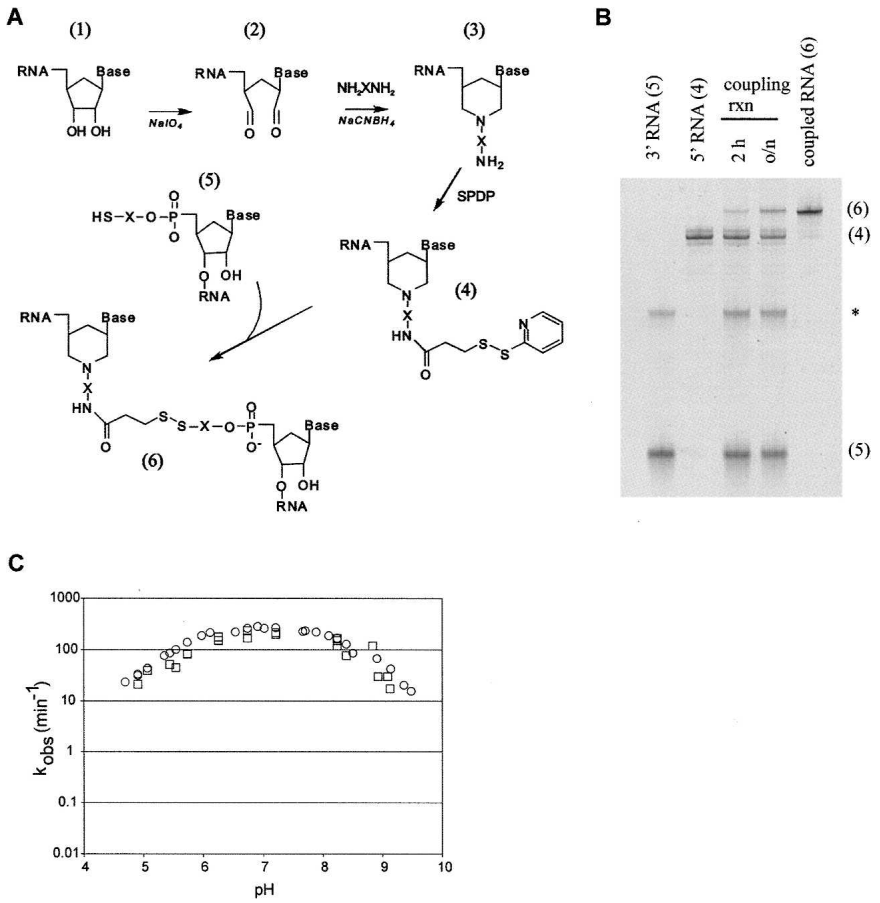

FIGURE 3. Mg^{2+}-independent RNA–RNA ligation scheme. (*A*) Synthesis scheme. Molecule 1, the upstream RNA, was synthesized by T7 transcription; molecule 4, the downstream RNA, was synthesized chemically and contains a nucleotide analog at position 638. X indicates a $(CH_2)_6$ linker, SPDP is N-succinimidyl 3-(2-pyridyldithiol)propionate, NH_2XNH_2 is hexamethylenediamine. (*B*) Denaturing PAGE analysis of typical input RNAs, a coupling reaction, and a gel-purified ligated precursor RNA from synthesis of RGssG (wild type); numbers in parentheses correspond to molecules numbered in the synthesis scheme; the asterisk indicates a presumed dimer of molecule 5. (*C*) Cleavage rate versus pH curve for RG RNA synthesized by in vitro transcription (circles; data from Fig. 1B) and RGssG prepared by the coupling scheme in *A* (squares).

disulfide linkage had no detrimental effect on the kinetics of *cis*-cleavage (Fig. 3C).

Base analog substitution at position 638

We used the above strategy to synthesize variants of RG in which G638 was replaced with purine nucleotide analogs with different functional groups and pK_a values (Fig. 4A). Chemically synthesized stem–loop I variant RNAs, equivalent to molecule 5 (Fig. 1A, boxed area) containing inosine (I), 2,6-diaminopurine (DAP), 2-aminopurine (2AP), or purine (P) at position 638 were joined via disulfide linkage to the remainder of the ribozyme that had been synthesized by T7 transcription and converted to the form of molecule 4 in Figure 3. The coupled, *cis*-cleaving ribozymes are designated RGssI, RGssDAP, RGss2AP, and RGssP, respectively.

Rate versus pH curves for the analog-containing RNAs are shown in Figure 4B. Below approximately pH 4 all RNAs examined showed the steep decrease in activity described above for wild type and 638A. In the pH range from about 4.5 to 9, where we could expect to observe indications of general acid–base catalysis, substitution with purine or 2AP caused slow, pH-independent cleavage; these analogs were not investigated further. Taken together with data described below, these observations suggest that the keto oxygen at position 6 of guanosine (and absent in purine and 2AP) and/or the protonation state of N1, whose pK_a would be several pH units lower in purine or 2AP compared to the natural guanosine, plays an important role in self-cleavage.

Substitution with inosine, which has only a slightly altered N1 pK_a compared to guanosine, but which lacks the 2-amino group, decreased the apparent cleavage rate by approximately an order of magnitude and shifted the rate versus pH curve slightly leftward, with apparent pK_as of 5.7 and 7.9. The small decrease in cleavage rate (compared to other analogs and the G638A mutant) and the small shift in apparent pK_as provide evidence that the 2-amino group of guanosine makes a measurable but small contribution to the self-cleavage reaction (see Discussion).

DAP, like adenosine, replaces the natural 6-keto group with an amino group, but the N1 pK_a of DAP is 1.3 units higher than adenosine. The rate versus pH curve of RGssDAP resembles that of 638A in showing a log-linear decrease in rate as pH increases, but the curve is shifted to a higher pH by about 1.5 pH units compared to adenosine. Like the 638A mutation, the RGssDAP curve can be described by a model in which steep loss in activity at low pH is combined with either general acid catalysis only or with general acid–base catalysis, with the curve shifted substantially downward and to the left compared to wild type. The latter model fits the data somewhat better, especially in that it yields values for n and pK_a^C that are similar to those for the other RNAs (Table 1, n = 6.5, pK_a^C = 4.0). Taken together, the effects of these base analog substitutions on the pH dependence of cleavage strongly support a role for G638 in the rate-limiting proton transfer step of the self-cleavage reaction.

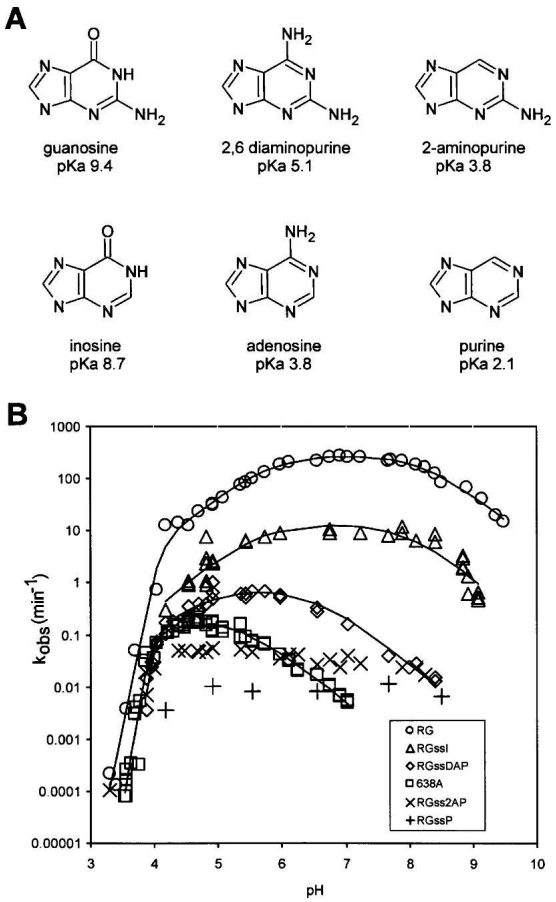

FIGURE 4. Effects of pH on cleavage rate of RNAs with purine analogs at position 638. (*A*) Nucleoside analogs and their N1 pK_a values (measured for the free nucleosides—actual pK_as in RNA may be different; Moody et al. 2005; Tang et al. 2007); the state of N1 protonation at neutral pH is shown. (*B*) Cleavage rate versus pH curves for wild-type RG (638G), mutant 638A, and RGss analog-containing RNAs containing inosine (RGssI), 2,6-diaminopurine (RGssDAP), 2-aminopurine (RGss2AP), and purine (RGssP) synthesized as in Figure 3A.

DISCUSSION

Site-specific base analog substitution in large ribozymes requires joining a chemically synthesized portion of RNA to the rest of the RNA to construct a self-cleaving precursor RNA with a base analog at a particular position. For many RNAs this has been accomplished using ligase enzymes that require divalent cations for activity. However, such enzymatic ligation strategies are not applicable to *cis*-cleaving ribozymes, especially those that cleave rapidly in divalent cations, because the precursor RNA formed by enzymatic ligation self-cleaves as fast as it is made. To overcome this problem we developed a method for joining two RNA molecules via a disulfide bond in the absence of divalent cations. The chemical ligation approach described here should be generally applicable to joining any two RNAs, or even constructing hybrid macromolecules composed of an RNA and another molecule containing a sulfhydryl group.

Using this approach we investigated the role in *cis*-cleavage of the nucleobase at position 638 in the cleavage loop of the VS ribozyme. Because some of the bases and base analogs used have low N1 pK_a values and we observed apparent pK_a s in the rate versus pH curves at low pH, a thorough analysis required measuring cleavage rates at pH values well below those typically collected when studying ribozymes. For all of the RNAs examined we observed a steep decrease in apparent cleavage rate below about pH 4.0. To obtain a mathematical description of the steep decrease in activity at low pH we fit the rate versus pH data for each RNA to a variety of models (see Materials and Methods and Results) that included a term involving some number, n, of bases with an average apparent pK_a, pK_a^C, which when protonated inactivated the ribozyme. The best fit was obtained with models in which the cooperative protonation of five to six bases, each with an average apparent pK_a^C of ~4.0, caused inactivation of the ribozyme.

Failure to include a term describing the steep decrease in activity at low pH can lead to misinterpretation of the remainder of the rate versus pH curve in certain situations. For example, a general acid-only reaction might be misinterpreted as a general acid–base reaction if data were not collected to a sufficiently low pH to correctly evaluate the decrease in activity below the apparent pK_a (see Fig. 1B). Even when data are collected at enough low pH values to describe the complete curve, it is still not possible to distinguish convincingly between a general acid-only model and a general acid–base model in the remainder of the curve if the putative lower pK_a of the general acid–base model has a value near pK_a^C; in this situation it is not even possible to accurately estimate the lower pK_a in the general acid–base model because the cooperative crash dominates the curve fitting in this region. For example, the cleavage curve of the 638A mutant RNA fits almost equally well to a general acid plus crash model as it does to a general acid–base plus crash model (Fig. 1B; Table 1).

The explanation for the steep decrease in activity at low pH is likely to involve loss of RNA structure. At low pH it would be expected that some adenine and cytosine bases in any RNA would become protonated, leading to loss of tertiary structure when a sufficient number of important interactions were disrupted, and even loss of secondary structure at sufficiently low pH (Moody et al. 2005; Siegfried et al. 2007). The apparent pK_a of 4.0 observed for the phenomenon causing the steep decline in activity of all of the RNA examined is consistent with protonation of adenosines and/or cytosines, which have pK_a s of ~3.8 and 4.2 as free nucleosides in solution that may be shifted slightly higher in the environment of a folded RNA (Saenger 1984; Moody et al. 2005). Similarly, a value of n = 5 or 6 seems a reasonable estimate for the number of protonatable bases that might be expected to disrupt the

tertiary interactions of an RNA of the size and complexity of the VS ribozyme. Known tertiary interactions in VS RNA include three Watson–Crick base pairs between loops I and V (Rastogi et al. 1996), a U-turn motif in the III–IV–V junction (Sood and Collins 2001), interactions in the II–III–VI junction (Lafontaine et al. 2001a), and between the cleavage site loop and the 730 loop (Hiley et al. 2002).

Our observations of the effects of base analogs at position 638 in the *cis*-cleaving RG version of the VS ribozyme are qualitatively similar to those recently reported by Lilley and coworkers (Wilson et al. 2007) using a *trans*-cleaving version of the ribozyme. Some of our interpretations are tempered by data that were not reported in that earlier study, including the effects of the steep loss of activity at low pH in the data analysis and rate versus pH data for two additional base analogs (purine and 2AP). Other differences in RNA design between the two studies likely account for some of the quantitative differences in apparent rates and pK_a values. For example, the substrate for the *trans* reaction used by Lilley and coworkers lacks helix Ia, which in *cis* affects the observed cleavage and ligation rates and the equilibrium between them (Rastogi and Collins 1998; Zamel et al. 2004; Smith and Collins 2007). In the current work, we used the RG version of the ribozyme that contains a stable helix Ia, additional nucleotides in the cleavage loop that strongly favor cleavage rather than ligation, and a G634C substitution that locks stem–loop Ib in the shifted conformation required for activity (Zamel et al. 2004). Despite these differences, a consistent story emerges from both studies that adds strong support to the hypothesis that G638 plays an important role in general acid–base catalysis in the VS ribozyme cleavage reaction.

In both *cis* and *trans* versions of the VS ribozyme, the removal of the exocyclic 2-amino group results in a leftward shift of the rate versus pH curve and a decrease in observed cleavage rate (compare guanosine with inosine and DAP with adenosine: the former of each pair contains the 2-amino group and has a slightly higher N1 pK_a; the latter lacks the 2-amino group) (Fig. 4). The magnitude of the rate decrease is about five- to 50-fold, depending on which version of the ribozyme and what pH is compared. This rather small decrease in rate suggests that the protons on the 2-amino group are not the ones transferred during the rate-limiting step, but that this exocyclic group may play a role in positioning or affecting the pK_a of the group involved in the rate-limiting step.

Removal of the keto oxygen has a severe effect on the observed cleavage rate. Comparing guanosine with 2AP, or inosine with purine, reveals a rate decrease of three to four orders of magnitude (Fig. 4). Even though these pairs of nucleotides differ structurally only by the presence or absence of the keto group, the absence of this group also leads to a decrease of about six pH units in the value of the N1 pK_a. From first principles of chemistry, and from studies of other ribozymes, the N1 position of guanosine is a likely candidate for participation in the chemical step of the reaction (Pinard et al. 2001; Kuzmin et al. 2004; Han and Burke 2005; Martick and Scott 2006; Thomas and Perrin 2006; Wilson et al. 2006), leaving open the possibility that the low N1 pK_a is responsible for the slow cleavage of the 2AP and purine substitutions.

Determining whether the decrease in activity of the 2AP and purine analogs is due mostly to the loss of the keto group or to the difference in N1 pK_a would benefit from a guanosine analog that retains the exocylic 2-amino and 6-keto groups but lacks a protonatable atom at ring position 1. To our knowledge an analog with these characteristics, such as N1 deazaguanosine, is not available. An 8-azaguanosine analog, whose fluorescence is affected by the state of N1 protonation (Da Costa et al. 2007), may also be a useful tool if it could be incorporated by chemical synthesis. As an alternative, rather than removing the keto group, we can compare the effects of replacing the keto group with an amino group. Comparing guanosine with DAP and inosine with adenosine shows that having an amino group instead of a keto group at ring position six is less deleterious than simply removing the keto group. As above, these exocyclic substitutions also alter the N1 pK_a. Indeed, observed cleavage rate follows the same order as N1 pK_a: guanosine is fastest, followed by inosine, DAP, and adenosine, in keeping with the possibility that N1 pK_a is an important determinant of the cleavage rate.

In both the VS and hairpin ribozymes, substitution of a putative catalytic guanosine nucleobase with an analog having a low pK_a produces a rate versus pH curve that is very different from that of wild type (Pinard et al. 2001; Wilson et al. 2007; this study). For example, substitution with adenosine or DAP results in very slow cleavage at higher pH, and the log of the cleavage rate constant increases linearly as pH decreases. This is in complete contrast to what is observed with the wild-type VS and hairpin ribozymes, in which cleavage is maximal at neutral pH and decreases as pH decreases in VS, or is pH-independent in the hairpin ribozyme. These observations suggest that the corresponding guanosines may play similar roles in the catalytic mechanisms of both ribozymes.

How much do the changes at position 638 affect the rate of the catalytic step of the self-cleavage reaction? This question is not as straightforward as it seems. A simple comparison of the relative maximum k_{obs} values provides one possible answer (Table 1, column 3); however, even in a simple model of the wild-type RNA in which the group with the apparent pK_a of 8.3 is assigned to G638 and the pK_a at 5.8 is assigned to A756, the principle of kinetic ambiguity shows that an alternative model in which these assignments are reversed is equally consistent with the observed cleavage rate data (Jencks 1969; Bevilacqua 2003). The two models differ substantially in their estimate of k_1, the intrinsic rate of catalysis, of wild type: 292 min^{-1} versus

93,600 min^{-1} (Fig. 5A,B; Table 1). When G638 is replaced with a base analog that has a different pK_a, we might have expected to see only one of the two apparent pK_a s in the rate versus pH curve change; however, in all cases, both apparent pK_a s were affected, indicating that analog substitutions have more widespread effects in the active site than simply altering only the pK_a of nucleotide 638. For example, there are two interpretations of the changes in pK_a in the DAP-containing RNA: (1) both of the wild-type pK_a s have shifted to lower values (8.3 to 6.5, and 5.8 to 4.8) or (2) the pK_a at 8.3 has shifted to 4.8 and the pK_a at 5.8 has moved upward to 6.5 (Fig. 5C,D). These two possible models, combined with each of the two kinetically ambiguous models for wild type, produce four possible answers to the question "how much slower is catalysis in the DAP-analog RNA" (Table 1).

In some cases we can argue that not all four of the possible answers are equally likely, as two of them require reversing the assignment of which pK_a is associated with the general acid and which with the general base. For example, inosine has a pK_a only slightly lower than guanosine, and the apparent pK_a s of the rate versus pH curve for the RNA containing inosine at position 638 (RGssI) are only slightly lower than in wild type. It seems most likely in this case that the apparent pK_a s of the two titratable groups in wild type have each simply shifted slightly lower, leading to the conclusion that k_1 in wild type is either 20-fold (comparing model 1 for each RNA) or 36-fold (comparing model 2) faster than in RGssI (not 6324-fold faster, nor the counterintuitive possibility that k_1 is actually faster in RGssI, as inferred from comparison of wild-type model 2 to mutant model 1 and vice versa, respectively; Table 1). On the other hand, the more dramatic changes in the rate versus pH curve for the adenosine- or DAP-containing RNAs make it difficult to tell which pK_a in the analog RNA corresponds to which in the wild type, leaving all four interpretations open, as well as the possibility (especially for the adenosine substitution) that the general base functionality has been eliminated.

A more quantitative comparison of intrinsic catalytic rates is further complicated by other factors that influence the estimation of k_1. The relationship between the observed cleavage rate and the theoretical maximal rate of a catalyzed reaction is described by $k_{obs} = F(k_1)$, where k_{obs} is the experimentally estimated apparent rate constant, k_1 is the intrinsic rate constant of the bond-breaking step, and F is the fraction of RNA in the catalytically competent state. As discussed previously (Bevilacqua 2003; Smith and Collins 2007), and expanded in the current work, F itself is the product of several proportions. These include $f_{HA+} \cdot f_{B-}$, which describes the fraction of the RNA population in which both the general acid and general base are in their functional protonated and deprotonated forms, respectively; and f_C, the proportion of RNA that retains critical tertiary interactions (this proportion decreases rapidly below approximately pH 4). Also implicit is a list of potential factors, up to f_n, describing the proportion of RNA in the correctly folded or docked state, the proportion in which putative electrostatic or transition state stabilizing interactions are formed, etc. So, at a given pH,

$$k_{obs} = (f_{HA+} \cdot f_{B-} \cdot f_C \cdot \ldots f_n) \cdot k_1$$

which implies that k_{obs} will have a much smaller value than the potential intrinsic rate of catalysis (k_1) that could be achieved if all of the RNA was in the catalytically competent state.

In summary, we present evidence that the N1 and/or 6-keto groups of the guanosine nucleotide at position 638 in the cleavage loop of the VS ribozyme are important for the rate-limiting proton transfer step in the *cis*-cleavage reaction catalyzed by this RNA. These experiments were made possible by a novel approach for joining two pieces of RNA in the absence of divalent cations via a disulfide bond. This approach should be applicable to the study of any RNA and to hybrid molecules consisting of an RNA joined to another sulfhydryl-containing molecule.

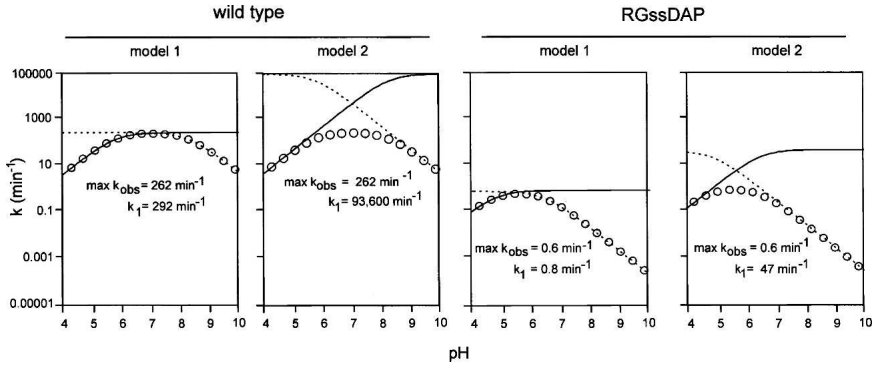

FIGURE 5. Estimation of k_1, the intrinsic rate of the bond-breaking step. Simulations of each of the two kinetically ambiguous models of general acid–base catalysis for wild-type and RGssDAP using Equations 3 and 4 in Materials and Methods (Bevilacqua 2003). Circles represent simulated k_{obs} values; dashed and dotted lines indicate the titration of the general acid or general base. Apparent pK_a values are summarized in Table 1.

MATERIALS AND METHODS

RNA constructs and mutants

The RG version of the VS ribozyme, derived from RS19 by including a C634G substitution that locks stem Ib in the shifted conformation required for activity (Andersen and Collins 2000), has been described previously (Smith and Collins 2007) and is shown in Figure 1A. Site-directed mutagenesis of the

ribozyme-encoding plasmid was used to construct mutants containing A, C, or U at position 638; sequences were confirmed by automated DNA sequencing of the entire ribozyme region. Precursor RNAs were obtained by in vitro transcription with T7 RNA polymerase in the presence of [α-^{32}P]GTP from plasmids linearized with EcoRI, followed by purification by denaturing gel electrophoresis and ethanol precipitation (Milligan et al. 1987; Hiley and Collins 2001).

Incorporation of base analogs was performed as outlined in Figure 3A. The 3′ RNA (molecule 5) was a chemically synthesized ribo-oligonucleotide obtained from Dharmacon, Inc. containing a base analog (Fig. 4A) at position 638 and a 5′ sulfhydryl group. The 5′ RNA was prepared by T7 RNA polymerase in vitro transcription from the RG plasmid template linearized with BglII; this yields an RNA whose 3′ end corresponds to the cytosine immediately upstream of the arrow indicated ''ss'' in Figure 1A (Fig. 3A, molecule 1). A representative procedure for the generation of RGss RNA is as follows. Molecule 1 ($\sim$1 μmol RNA), was oxidized with 10 mM sodium periodate in 50 mM sodium acetate (pH 4.8) in a 50 μL volume. Reactions were incubated at room temperature for 30 min and then filtered through a micro G50 column (ProbeQuant G-50 Micro Column GE Healthcare) equilibriated in 5 mM sodium phosphate (pH 7.2) and ethanol precipitated. The 3′ amine was introduced into the oxidized RNA via reductive amination. The oxidized RNA was treated with 40 mM hexamethylenediamine dihydrochloride and 10 mM sodium cyanoborohydride in 50 mM sodium acetate (pH 4.8) in a 50 μL volume. Reactions were incubated at room temperature for 2 h and then filtered through a micro G50 column and ethanol precipitated. The activated thiol was introduced via the 3′ amine RNA using 1 mM N-succinimidyl 3-(2-pyridyldithio) propionate (SPDP; Pierce Scientific) in 10 mM sodium phosphate (pH 7.2), 150 mM NaCl, and 1 mM EDTA. Reactions were incubated at room temperature for 2 h and then filtered through a micro G50 column and ethanol precipitated. Molecule 5 was deprotected by treatment with 40 mM DTT in 10 mM sodium phosphate (pH 7.2), 150 mM NaCl, and 1 mM EDTA. After a 2-h incubation at room temperature, the DTT was removed by passing the reaction through a micro G50 column. The upstream and downstream RNAs (5 μM and 30 μM, respectively) were coupled via thiol exchange in 10 mM sodium phosphate (pH 7.2), 150 mM NaCl, and 1 mM EDTA. After overnight incubation at 4°C the reactions were quenched by addition of 2× the reaction volume of formamide RNA loading dye. RNAs were separated by electrophoresis on a 4% polyacrylamide/ 8.3 M urea gel, excised, and eluted into 2 mL of water (65°C, 1 h). Eluted RNAs were filtered through 0.8 μm/0.2 μmM Acrodiscs (Gelman Sciences). The RNAs were then ethanol precipitated and dissolved in water. The RNA concentrations for the coupling step have not been fully optimized; typical yields from the coupling step ranged from 5% to 63%. Typical reactions starting with 1 μmol of upstream RNA give rise to 50–200 pmol of purified coupled RNA.

Cis-cleavage reactions

Buffers used were lactate, acetate, MES, cacodylate, Tris, HEPES, and CAPSO. pH was adjusted by titration with NaOH or HCl; in some cases mixtures of two buffers were used to obtain the desired pH. Because the high concentration of $MgCl_2$ affected the pH of the different buffered solutions and their concentrated stocks to different extents, pH values reported are those for 1× solutions containing all components except RNA measured at 37°C with a SympHony pH meter and calomel microelectrode (VWR Scientific Products) calibrated at 37°C. RNA was preincubated at 37°C in 1× reaction solution (40 mM buffer, 50 mM KCl, 2 mM spermidine). Reactions were initiated by mixing one volume of RNA with one volume of pre-warmed 1× reaction solution containing 400 mM $MgCl_2$ (final concentrations of $MgCl_2$ and RNA = 200 mM and 10 nM, respectively) either by manual pipetting or using a Kintek RQF-3 rapid quench flow instrument (Kintek Corp.), stopped, and analyzed by gel electrophoresis and Phosphorimaging as described previously (Smith and Collins 2007).

Data analysis

Data from individual self-cleavage reaction time courses were fit to a single exponential:

$$f_c = f_{\max}(e^{-kt}), \tag{1}$$

where f_c is the fraction cleaved at time t, k is the apparent cleavage rate constant k_{obs}, and f_{max} is the fraction of the RNA that was cleavable. Between pH $\approx$ 5.5 and 4.0, cleavage curves for RG RNA became biphasic, with a decreasing fraction of RNA in the fast phase as pH decreased. In this pH region the rate of the data were fit to a double exponential:

$$f_c = f_{\max}(A_1 \cdot e^{-k_1 t} + A_2 \cdot e^{-k_2 t}), \tag{2}$$

where A_1 and A_2 are the amplitudes and k_1 and k_2 are the rate constants of the fast and slow phase, respectively. The rate constant of the fast phase, k_1, was used for subsequent analyses; k_2 was several 100-fold slower than k_1 and has not been investigated further.

Estimation of parameters from rate versus pH curves

The intrinsic rate constant of the bond-breaking step, k_1, is related to the experimentally observed apparent rate constant, k_{obs}, by

$$k_{\text{obs}} = f_{\text{active}} \cdot k_1, \tag{3}$$

where f_{active} is the fraction of RNA in the functional state to perform catalysis (see below). The fraction of RNA in the protonation state capable of general acid–base or general acid-only catalysis (f_{ab} or f_a, respectively) is described by Equation 4 or 5.

General acid–base catalysis (Bevilacqua 2003):

$$f_{ab} = f_{HA+} \cdot f_{B-} = 1/(1 + 10^{(\mathrm{p}K_a{}^B - \mathrm{pH})} + 10^{(\mathrm{p}K_a{}^B - \mathrm{p}K_a{}^A)} + 10^{(\mathrm{pH} - \mathrm{p}K_a{}^A)}), \tag{4}$$

General acid-only catalysis:

$$f_a = f_{HA+} = 1/(1 + 10^{(\mathrm{pH} - \mathrm{p}K_a{}^A)}), \tag{5}$$

where f_{HA+} and f_{B-} are the fractions of the RNA population in which the general acid and general base are protonated and

deprotonated, respectively; pK_a^A and pK_a^B are the apparent pK_a of the general acid and base.

To model the steep decrease in k_{obs} at low pH, the following two equations were evaluated to describe the fraction of RNA in the active state due to pH-dependent inactivation of the ribozyme by a process independent of general acid–base catalysis.

Protonation of multiple independent sites (Knitt and Herschlag 1996):

$$f_i = 1/(1 + 10^{(pK_a^C - pH)})^n, \quad (6)$$

Or cooperative protonation of multiple sites (derived from the Hill equation; Weiss 1997):

$$f_c = 1/1 + (10^{(pK_a^C - pH)})^n, \quad (7)$$

where f_i or f_c is the fraction of active RNA, n is the number, and pK_a^C is the average apparent pK_a of nucleotides that must be protonated for the RNA to lose activity at low pH. Equation 7, but not Equation 6, provided an adequate fit to the data (see Results).

To calculate the fraction of active RNA, f_{active}, at any point in the pH range, Equation 4 or 5 (which describe the fraction of RNA in the appropriate protonation state for general acid or general acid–base catalysis) was multiplied by Equation 7 (which describes the fraction of RNA in the active state affected by the low pH inactivation). For example, the wild-type data are best described by a combination of general acid–base catalysis and loss of activity by cooperative protonation at low pH:

$$f_{active} = f_{ab} \cdot f_c = [1/(1 + 10^{(pK_a^B - pH)} + 10^{(pK_a^B - pK_a^A)} + 10^{(pH - pK_a^A)})] \cdot [1/1 + (10^{(pK_a^C - pH)})^n].$$

k_{obs} versus pH data were fit to versions of Equation 3 where f_{active} was described by combining Equations 4 and 7 or Equations 5 and 7. To equalize the weighting of all data points, nonlinear least squares curve fitting was performed using the natural logarithm of k_{obs}, using the Solver add-in of Microsoft Excel 2003 (Microsoft Corp.) to simultaneously estimate optimal values of k_1, pK_a^A, pK_a^B, pK_a^C, and n.

ACKNOWLEDGMENTS

This research was supported by the Canadian Institutes for Health Research and the Canada Foundation for Innovation.

Received November 22, 2007; accepted January 21, 2008.

REFERENCES

Andersen, A.A. and Collins, R.A. 2000. Rearrangement of a stable RNA secondary structure during VS ribozyme catalysis. *Mol. Cell* **5:** 469–478.

Baum, D.A. and Silverman, S.K. 2007. Deoxyribozyme-catalyzed labeling of RNA. *Angew. Chem. Int. Ed. Engl.* **46:** 3502–3504.

Bellon, L., Workman, C., Scherrer, J., Usman, N., and Wincott, F. 1996. Morpholino-linked ribozymes: A convergent synthetic approach. *J. Am. Chem. Soc.* **118:** 3771–3772.

Bevilacqua, P.C. 2003. Mechanistic considerations for general acid–base catalysis by RNA: Revisiting the mechanism of the hairpin ribozyme. *Biochemistry* **42:** 2259–2265.

Bevilacqua, P.C., Brown, T.S., Nakano, S., and Yajima, R. 2004. Catalytic roles for proton transfer and protonation in ribozymes. *Biopolymers* **73:** 90–109.

Cohen, S.B. and Cech, T.R. 1997. Dynamics of thermal motions within a large catalytic RNA investigated by cross-linking with thiol-disulfide interchange. *J. Am. Chem. Soc.* **119:** 6259–6268.

Curtis, E.A. and Bartel, D.P. 2001. The hammerhead cleavage reaction in monovalent cations. *RNA* **7:** 546–552.

Da Costa, C.P., Fedor, M.J., and Scott, L.G. 2007. 8-Azaguanine reporter of purine ionization states in structured RNAs. *J. Am. Chem. Soc.* **129:** 3426–3432.

Das, S.R. and Piccirilli, J.A. 2005. General acid catalysis by the hepatitis delta virus ribozyme. *Nat. Chem. Biol.* **1:** 45–52.

Eckstein, F. 1985. Nucleoside phosphorothioates. *Annu. Rev. Biochem.* **54:** 367–402.

Fedor, M.J. and Williamson, J.R. 2005. The catalytic diversity of RNAs. *Nat. Rev. Mol. Cell Biol.* **6:** 399–412.

Han, J. and Burke, J.M. 2005. Model for general acid–base catalysis by the hammerhead ribozyme: pH-activity relationships of G8 and G12 variants at the putative active site. *Biochemistry* **44:** 7864–7870.

Hiley, S.L. and Collins, R.A. 2001. Rapid formation of a solvent-inaccessible core in the Neurospora Varkud satellite ribozyme. *EMBO J.* **20:** 5461–5469.

Hiley, S.L., Sood, V.D., Fan, J., and Collins, R.A. 2002. 4-thio-U cross-linking identifies the active site of the VS ribozyme. *EMBO J.* **21:** 4691–4698.

Hoffmann, B., Mitchell, G.T., Gendron, P., Major, F., Andersen, A., Collins, R.A., and Legault, P. 2003. NMR structure of the active conformation of the Varkud satellite ribozyme cleavage site. *Proc. Natl. Acad. Sci.* **100:** 7003–7008.

Jencks, W. 1969. *Catalysis and enzymology*: Dover Publications Inc., New York.

Jones, F.D. and Strobel, S.A. 2003. Ionization of a critical adenosine residue in the *Neurospora* Varkud satellite ribozyme active site. *Biochemistry* **42:** 4265–4276.

Ke, A., Zhou, K., Ding, F., Cate, J.H., and Doudna, J.A. 2004. A conformational switch controls hepatitis δ virus ribozyme catalysis. *Nature* **429:** 201–205.

Knitt, D.S. and Herschlag, D. 1996. pH dependencies of the *Tetrahymena* ribozyme reveal an unconventional origin of an apparent pK_a. *Biochemistry* **35:** 1560–1570.

Kuzmin, Y.I., Da Costa, C.P., and Fedor, M.J. 2004. Role of an active site guanine in hairpin ribozyme catalysis probed by exogenous nucleobase rescue. *J. Mol. Biol.* **340:** 233–251.

Lafontaine, D.A., Norman, D.G., and Lilley, D.M. 2001a. Structure, folding and activity of the VS ribozyme: Importance of the 2-3-6 helical junction. *EMBO J.* **20:** 1415–1424.

Lafontaine, D.A., Wilson, T.J., Norman, D.G., and Lilley, D.M. 2001b. The A730 loop is an important component of the active site of the VS ribozyme. *J. Mol. Biol.* **312:** 663–674.

Lafontaine, D.A., Wilson, T.J., Zhao, Z.Y., and Lilley, D.M. 2002. Functional group requirements in the probable active site of the VS ribozyme. *J. Mol. Biol.* **323:** 23–34.

Martick, M. and Scott, W.G. 2006. Tertiary contacts distant from the active site prime a ribozyme for catalysis. *Cell* **126:** 309–320.

Milligan, J.F., Groebe, D.R., Witherell, G.W., and Uhlenbeck, O.C. 1987. Oligoribonucleotide synthesis using T7 RNA polymerase and synthetic DNA templates. *Nucleic Acids Res.* **15:** 8783–8798. doi: 10.1093/nar/15.21.8783.

Moody, E.M., Lecomte, J.T., and Bevilacqua, P.C. 2005. Linkage between proton binding and folding in RNA: A thermodynamic framework and its experimental application for investigating pK_a shifting. *RNA* **11:** 157–172.

Moore, M.J. and Query, C.C. 2000. Joining of RNAs by splinted ligation. *Methods Enzymol.* **317:** 109–123.

Moore, M.J. and Sharp, P.A. 1992. Site-specific modification of pre-mRNA: The 2′-hydroxyl groups at the splice sites. *Science* **256:** 992–997.

Murray, J.B., Seyhan, A.A., Walter, N.G., Burke, J.M., and Scott, W.G. 1998. The hammerhead, hairpin and VS ribozymes are catalytically proficient in monovalent cations alone. *Chem. Biol.* **5:** 587–595.

Nakano, S., Chadalavada, D.M., and Bevilacqua, P.C. 2000. General acid–base catalysis in the mechanism of a hepatitis δ virus ribozyme. *Science* **287:** 1493–1497.

Nesbitt, S., Hegg, L.A., and Fedor, M.J. 1997. An unusual pH-independent and metal-ion-independent mechanism for hairpin ribozyme catalysis. *Chem. Biol.* **4:** 619–630.

Ogilvie, K.K., Usman, N., Nicoghosian, K., and Cedergren, R.J. 1988. Total chemical synthesis of a 77-nucleotide-long RNA sequence having methionine-acceptance activity. *Proc. Natl. Acad. Sci.* **85:** 5764–5768.

O'Rear, J.L., Wang, S., Feig, A.L., Beigelman, L., Uhlenbeck, O.C., and Herschlag, D. 2001. Comparison of the hammerhead cleavage reactions stimulated by monovalent and divalent cations. *RNA* **7:** 537–545.

Perrotta, A.T. and Been, M.D. 2006. HDV ribozyme activity in monovalent cations. *Biochemistry* **45:** 11357–11365.

Perrotta, A.T., Wadkins, T.S., and Been, M.D. 2006. Chemical rescue, multiple ionizable groups, and general acid–base catalysis in the HDV genomic ribozyme. *RNA* **12:** 1282–1291.

Pinard, R., Hampel, K.J., Heckman, J.E., Lambert, D., Chan, P.A., Major, F., and Burke, J.M. 2001. Functional involvement of G8 in the hairpin ribozyme cleavage mechanism. *EMBO J.* **20:** 6434–6442.

Poon, A.H., Olive, J.E., McLaren, M., and Collins, R.A. 2006. Identification of separate structural features that affect rate and cation concentration dependence of self-cleavage by the *Neurospora* VS ribozyme. *Biochemistry* **45:** 13394–13400.

Pyle, A.M. 1993. Ribozymes: A distinct class of metalloenzymes. *Science* **261:** 709–714.

Rastogi, T. and Collins, R.A. 1998. Smaller, faster ribozymes reveal the catalytic core of *Neurospora* VS RNA. *J. Mol. Biol.* **277:** 215–224.

Rastogi, T., Beattie, T.L., Olive, J.E., and Collins, R.A. 1996. A long-range pseudoknot is required for activity of the *Neurospora* VS ribozyme. *EMBO J.* **15:** 2820–2825.

Saenger, W. 1984. *Principles of nucleic acid structure*. Springer-Verlag, New York.

Scaringe, S.A., Francklyn, C., and Usman, N. 1990. Chemical synthesis of biologically active oligoribonucleotides using β-cyanoethyl protected ribonucleoside phosphoramidites. *Nucleic Acids Res.* **18:** 5433–5441. doi: 10.1093/nar/18.18.5433.

Shih, I.H. and Been, M.D. 2001. Involvement of a cytosine side chain in proton transfer in the rate-determining step of ribozyme self-cleavage. *Proc. Natl. Acad. Sci.* **98:** 1489–1494.

Siegfried, N.A., Metzger, S.L., and Bevilacqua, P.C. 2007. Folding cooperativity in RNA and DNA is dependent on position in the helix. *Biochemistry* **46:** 172–181.

Sigel, R.K. and Pyle, A.M. 2007. Alternative roles for metal ions in enzyme catalysis and the implications for ribozyme chemistry. *Chem. Rev.* **107:** 97–113.

Smith, M.D. and Collins, R.A. 2007. Evidence for proton transfer in the rate-limiting step of a fast-cleaving Varkud satellite ribozyme. *Proc. Natl. Acad. Sci.* **104:** 5818–5823.

Sood, V.D. and Collins, R.A. 2001. Functional equivalence of the uridine turn and the hairpin as building blocks of tertiary structure in the *Neurospora* VS ribozyme. *J. Mol. Biol.* **313:** 1013–1019.

Sood, V.D. and Collins, R.A. 2002. Identification of the catalytic subdomain of the VS ribozyme and evidence for remarkable sequence tolerance in the active site loop. *J. Mol. Biol.* **320:** 443–454.

Strobel, S.A. 1999. A chemogenetic approach to RNA function/structure analysis. *Curr. Opin. Struct. Biol.* **9:** 346–352.

Tang, C.L., Alexov, E., Pyle, A.M., and Honig, B. 2007. Calculation of pK_as in RNA: On the structural origins and functional roles of protonated nucleotides. *J. Mol. Biol.* **366:** 1475–1496.

Thomas, J.M. and Perrin, D.M. 2006. Active site labeling of G8 in the hairpin ribozyme: Implications for structure and mechanism. *J. Am. Chem. Soc.* **128:** 16540–16545.

Weiss, J.N. 1997. The Hill equation revisited: Uses and misuses. *FASEB J.* **11:** 835–841.

Wilson, T.J., Ouellet, J., Zhao, Z.Y., Harusawa, S., Araki, L., Kurihara, T., and Lilley, D.M. 2006. Nucleobase catalysis in the hairpin ribozyme. *RNA* **12:** 980–987.

Wilson, T.J., McLeod, A.C., and Lilley, D.M. 2007. A guanine nucleobase important for catalysis by the VS ribozyme. *EMBO J.* **26:** 2489–2500.

Wincott, F., DiRenzo, A., Shaffer, C., Grimm, S., Tracz, D., Workman, C., Sweedler, D., Gonzalez, C., Scaringe, S., and Usman, N. 1995. Synthesis, deprotection, analysis and purification of RNA and ribozymes. *Nucleic Acids Res.* **23:** 2677–2684. doi: 10.1093/nar/23.14.2677.

Young, K.J., Gill, F., and Grasby, J.A. 1997. Metal ions play a passive role in the hairpin ribozyme catalysed reaction. *Nucleic Acids Res.* **25:** 3760–3766. doi: 10.1093/nar/25.19.3760.

Zamel, R., Poon, A., Jaikaran, D., Andersen, A., Olive, J., De Abreu, D., and Collins, R.A. 2004. Exceptionally fast self-cleavage by a *Neurospora* Varkud satellite ribozyme. *Proc. Natl. Acad. Sci.* **101:** 1467–1472.